



## Sweet triterpenoid glycoside from *Cyclocarya paliurus* ameliorates obesity-induced insulin resistance through inhibiting the TLR4/NF- $\kappa$ B/NLRP3 inflammatory pathway

Jie Li <sup>a,1</sup>, Junyu He <sup>b,1</sup>, Haibo He <sup>a,c,\*</sup>, Xiao Wang <sup>a</sup>, Shuran Zhang <sup>a</sup>, Yumin He <sup>b,\*\*</sup>, Jihong Zhang <sup>d</sup>, Chengfu Yuan <sup>b</sup>, HongWu Wang <sup>e,\*\*\*</sup>, Daoxiang Xu <sup>f</sup>, Chaowang Pan <sup>g</sup>, Huifan Yu <sup>c</sup>, Kun Zou <sup>a</sup>

<sup>a</sup> Hubei Key Laboratory of Natural Products Research and Development & Yichang Key Laboratory of Development and Utilization of Health Products with Drug and Food Homology, China Three Gorges University, Yichang, Hubei, 443002, China

<sup>b</sup> Basic Medical College of China Three Gorges University, Yichang, Hubei, 443002, China

<sup>c</sup> Hubei Key Laboratory of Wudang Local Chinese Medicine Research, Hubei University of Medicine, Shiyan, Hubei, 442000, China

<sup>d</sup> Traditional Chinese Medicine Hospital of China Three Gorges University & Hubei Clinical Research Center for Functional Digestive Diseases of Traditional Chinese Medicine, Yichang, Hubei, 443001, China

<sup>e</sup> Department and Institute of Infectious Disease, Tongji Hospital, Tongji Medical College, Hua Zhong University of Science and Technology, Wuhan, 430030, China

<sup>f</sup> Seventh People's Hospital of Wenzhou, Wenzhou, Zhejiang, 325005, China

<sup>g</sup> Medical College of Ezhou Vocational University, Ezhou, Hubei, 436000, China

### ARTICLE INFO

Handling editor: Quancai Sun

#### Keywords:

Leaves of *Cyclocarya paliurus*  
Sweet triterpenoid glycoside  
Insulin resistance  
TLR4/NF- $\kappa$ B/NLRP3 signaling pathway

### ABSTRACT

Our prophase studies have manifested that the sweet triterpenoid glycoside from the leaves of *Cyclocarya paliurus* (CPST) effectively improved the disorders of glucolipid metabolism *in vitro* and in patients. The current purpose was to further detect its mechanisms involved. The results demonstrated that CPST could ameliorate high-fat diet (HFD)-induced insulin resistance (IR), which was linked to reducing HFD-induced mice's body weight, serum glucose (GLUO), triglyceride (TG), total cholesterol (T-CHO) and low-density lipoprotein cholesterol (LDL-C), lowering the area under the oral glucose tolerance curve and insulin tolerance, elevating the percentage of brown adipose, high-density lipoprotein cholesterol (HDL-C), reducing fat droplets of adipocytes in interscapular brown adipose tissue (iBAT) and cross-sectional area of adipocytes. Further studies manifested that CPST obviously downregulated TLR4, MyD88, NLRP3, ASC, caspase-1, cleaved-caspase-1, IL-18, IL-1 $\beta$ , TXNIP, and GSDMD protein expressions and p-NF- $\kappa$ B/NF- $\kappa$ B ratio in iBAT. These aforementioned findings demonstrated that CPST ameliorated HFD induced IR by regulating TLR4/NF- $\kappa$ B/NLRP3 signaling pathway, which in turn enhancing insulin sensitivity and glucose metabolism.

### 1. Introduction

Nowadays, with the gradual improvement of the national living standard and the acceleration of the pace of life, the modern lifestyle of high intake and low consumption have become very widespread (He et al., 2020). As a result, dietary obesity and various metabolic diseases caused by it, such as insulin resistance (IR), type 2 diabetes (T2D)

(Tanase et al., 2020), non-alcoholic fatty liver, atherosclerosis, hypertension, etc., are becoming the main threat to people's health worldwide, which is closely related to the excessive accumulation of adipose tissue and energy imbalance (Natur et al., 2022; Rangel-Azevedo et al., 2022; Yu et al., 2021). As everyone knows, white adipose tissue (WAT) acts as a secretory organ to regulate insulin sensitivity and maintain energy metabolic homeostasis, while brown adipose tissue (BAT) is an

\* Corresponding author. Hubei Key Laboratory of Natural Products Research and Development & Yichang Key Laboratory of Development and Utilization of Health Products with Drug and Food Homology, China Three Gorges University, Yichang, Hubei, 443002, China.

\*\* Corresponding author.

\*\*\* Corresponding author.

E-mail addresses: [hehaibo252219@163.com](mailto:hehaibo252219@163.com) (H. He), [hym0811@163.com](mailto:hym0811@163.com) (Y. He), [hongwuwang@126.com](mailto:hongwuwang@126.com) (H. Wang).

<sup>1</sup> These authors contributed equally for this work.

energy-consuming tissue which maintains body temperature and energy homeostasis through thermogenesis (Boström et al., 2012; Kim et al., 2022; Wu et al., 2012; Xuan et al., 2022). Recent studies have revealed that their distributions are not independent of each other, many stimuli, such as cold and agonists, can promote the transformation of WAT into BAT, also named white adipocyte browning (Jiang et al., 2022; Scarano et al., 2021). The white adipocytes browned has a high thermogenic efficiency, which can rapidly consume energy and promote lipid metabolism, so accelerating the browning process of WAT is considered a new strategy for the effective treatment of obesity (Monfort-Pires et al., 2022).

An increasing body of evidence suggests that the adipose tissue is considered to be one of the most important endocrine organs involved in the regulation of the inflammatory response, closely related to the inflammation caused by obesity (Gonzalez-Muniesa et al., 2017; Jorquera et al., 2021; Kojta et al., 2020), which is the main cause of IR and other obesity related metabolic diseases (Roberts-Toler, O'Neill and Cypess, 2015). In recent years, scholars have found that the activated toll like receptor 4/nuclear factor  $\kappa$ B/NOD like receptor protein 3 (TLR4/NF- $\kappa$ B/NLRP3) signaling pathway plays an extremely important role in the inflammatory activation of adipose tissue and the expression and secretion of inflammatory mediators and inflammatory factors (Griffin et al., 2018; Lu et al., 2022; Sánchez-Tapia et al., 2019). On the one hand, a large number of fat factors and saturated fatty acids generated in patients of obesity-induced IR can boost TLR4, and promote NF- $\kappa$ B activation, increase the expressions of tumor necrosis factor- $\alpha$  (TNF- $\alpha$ ) and interleukin-1 $\beta$  (IL-1 $\beta$ ), etc. proinflammatory cytokines in WAT/BAT promote the formation of WAT, and affect glucose uptake and fatty acid metabolism (Benomar et al., 2016; Kumari et al., 2016; Ono-Moore et al., 2017); On the other hand may activate NLRP3 inflammasome, and its activation lead to activation of caspase-1 and releases of IL-1 $\beta$  and IL-18. All of these indicated that the related protein expressions of NLRP3 inflammasome were significantly elevated in adipose tissue from obese, dyslipidemic, and diabetic patients and positively correlated with the severity of IR (Jourdan et al., 2013; Zhang et al., 2021). Therefore, promoting the browning of WAT to BAT and intervening the TLR4/NF- $\kappa$ B/NLRP3 signaling pathway in BAT of obesity-induced IR patients is of great significance in regulating dyslipidemia and improving the inflammatory state of adipose tissue for the prevention and treatment of obesity-induced IR.

*Cycocarya paliurus* (Batal) Iljinskaja (*C. paliurus*), also known as “sweet tea tree”, “money tree”, is a deciduous tree of the genus *Cycocarya* in the dicotyledonaceae family and a monocotyledonous genus endemic to China, as well as a new food raw material recognized by the National Health Commission (Liu et al., 2017, 2018). According to the records in “Chinese Traditional Medicine Resources”, the leaves, bark, and roots of *C. paliurus* can be used as traditional Chinese medicine, which is warm, pungent, and slightly bitter, and has the function of clearing heat, reducing swelling and relieving pain, and can be used to treat ringworm. Because of the sweet taste of its leaves, as well as its excellent effect on lowering lipids, sugar and blood pressure, it is known as “divine tea”, and the “third tree” in the medical field. Studies on chemical constituents demonstrated its main components are triterpenoids, flavonoids, polysaccharides, phenylpropionic acid, and so forth, which has the traditional effect of dispelling wind and relieving itching (Wang et al., 2018; Xiong et al., 2018; Zhao et al., 2022). Modern pharmacological researches have demonstrated that *C. paliurus* is used to treat diabetes, hyperlipidemia, hypertension and other three high diseases. At the same time, it also has the effects of pain relief, anti-inflammatory, anti-tumor, and improving immunity (Fang et al., 2019; Feng et al., 2021; Lin et al., 2021; Liu et al., 2020; Zhao et al., 2021; Wang et al., 2016; Wang et al., 2022; Wang et al., 2020; Wu et al., 2020; Wu et al., 2021). Our prophase studies have manifested that the sweet triterpenoid glycoside from the leaves of *C. paliurus* (CPST) revealed good therapeutic effects on the disorders of glucolipid metabolism *in vitro* and in patients, and further verified that inhibiting the

abnormal expression and secretion of inflammatory mediators and inflammatory factors were closely related to ameliorating obesity-induced IR (Qin et al., 2016; He et al., 2021a,b; He et al., 2021; Zhou et al., 2016). However, its potential molecular mechanisms have not been fully enlightened.

Based on the central player of TLR4/NF- $\kappa$ B/NLRP3 inflammatory pathway in ameliorating obesity-induced IR, and therapeutic effects on the disorders of glucolipid metabolism in our prophase studies, the current study was to further detect its therapeutic effects on BAT in obesity-induced IR mice, and its potential mechanisms through modulating TLR4/NF- $\kappa$ B/NLRP3 signaling pathway, which would lay a foundation for expanding the application range of the leaves of *C. paliurus* and developing sophisticated products in the future.

## 2. Materials and methods

### 2.1. Plant material

*C. paliurus* leaves in April 2021 were purchased from Quanzhou Qingqianliu Planting Base (Guangxi, China), and were identified by professor Yubing Wang, China Three Gorges University. Voucher specimens (2021-0426) are deposited in the Yichang Key Laboratory of Development and Utilization of Health Products with Drug and Food Homology, College of Biological and Pharmaceutical Sciences, China Three Gorges University.

### 2.2. Reagents

All solvents used for the extraction and analysis of CPST in our study were of analytical grade and obtained from Sinopharm Chemical Reagent Co., Ltd (Shanghai, China). Agilent XB C18 column was purchased from Agilent Technologies, USA. RIPA lysate, phosphatase inhibitors and PMSF were obtained from Beijing Solarbio Science Technology Co., Ltd. (Beijing, China). BCA protein concentration determination kit was purchased from Beyotime Biotechnology (Nanjing, China). Rabbit anti mouse myeloid differentiation primary response gene 88 (MyD88), NF- $\kappa$ Bp65, p-NF- $\kappa$ Bp65, NLRP3, apoptosis associated speck like protein containing CARD (ASC), caspase-1, cleaved caspase-1, IL-18, IL-1 $\beta$ , gasdermin-D (GSDMD) and uncoupling protein 1 (UCP1) were obtained from Cell Signaling Technology (MA, USA). Rabbit anti mouse thioredoxin-interacting protein (TXNIP) was purchased from Affinity Bioreagents (MA, USA). Rabbit anti-mouse TLR4 and  $\beta$ -actin were obtained from AB clonal Biotechnology (Wuhan, China). All primary antibody dilutions were 1:1000. WesternBright ECL prime detection reagent, SDS-PAGE gel kit, PVDF membrane were obtained from Boshide Biotechnology Company (Wuhan, China). Other reagents used in the present study were of analytical grade.

### 2.3. Extraction of CPST

5.0 kg of dry *C. paliurus* leaves were accurately weighed, and added 50.0 L of lime water with a pH of 13, was soaked at room temperature for 1 h, filtered, and discarded. Washing the filtrate with clean water three times until the pH test paper was neutral. Then, 20 times 70% ethanol was added for reflux extraction for 2 h and repeated four times. The liquid after centrifugal filtration is the ethanol extract, and eluting it with ten times water of the column volume, 20% ethanol, and 80% ethanol through the macroporous adsorption resin (Brand: X-5, specification: 500 g, loading amount: 4.0 L, size: diameter 100 mm, length 800 mm). We collected the 80% ethanol eluent and recovered the ethanol under pressure to obtain the 80% ethanol elution site. Then the parts were dispersed with 1.0 L water and extracted with 4.0 L ethyl acetate. After recovering the solvent, we obtained the ethyl acetate parts that we defined as CPST.

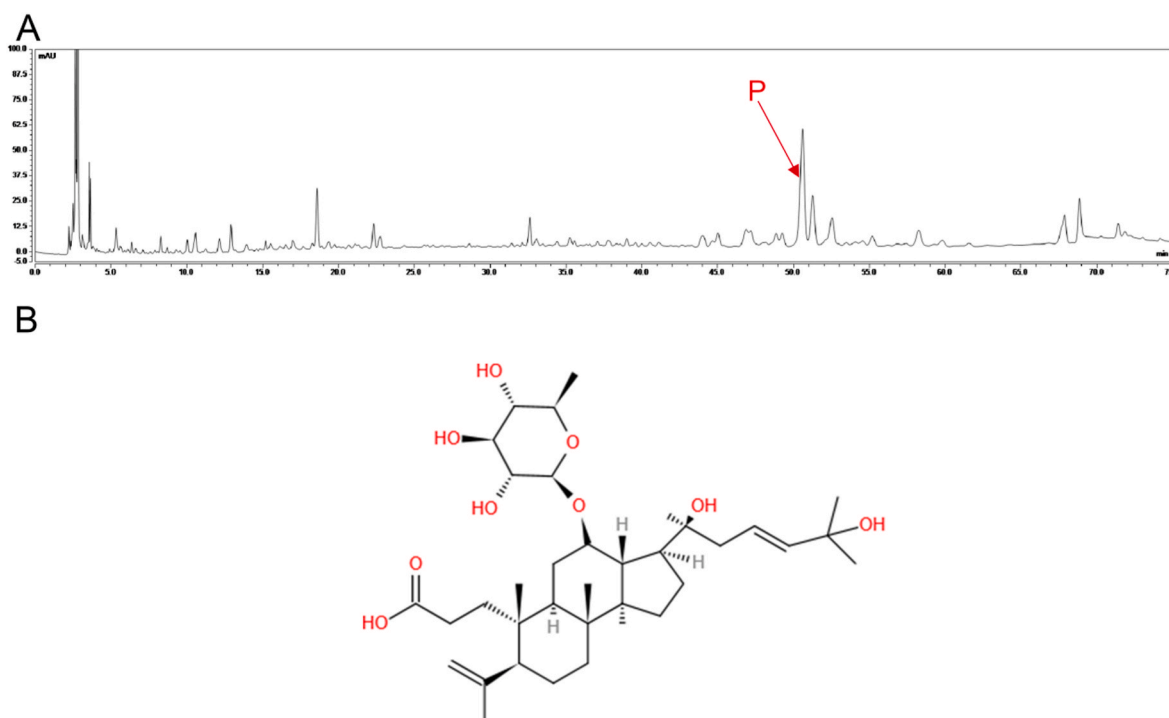


**Fig. 1.** The chromatogram and chemical structures of pterocaryoside B obtained from *C. paliurus* leaves. (A) The HPLC analysis of CPST, position P is pterocaryoside B. (B) Chemical structures of pterocaryoside B.

#### 2.4. Pterocaryoside B determination in CPST

In our previous research, we isolated and identified a monomeric compound from the CPST as pterocaryoside B with strong sweetness, which is structurally characterized by a dammarane-type triterpene parent nucleus with a 2,3-position cleavage ring, containing two unsaturated double bonds and connected to an is arabinose ligand, consistent with the characteristics of the main component contained in the defined *C. paliurus* sweet triterpenoid. Therefore, this paper determined the content of pterocaryoside B by high performance liquid chromatography (HPLC) for the CPST prepared by the above means. The analysis of the plant extracts was performed according to a previously reported method with minor modifications. Briefly, the appropriate amounts of CPST samples were weighed separately and precisely into conical flasks, sonicated with chromatographic grade methanol for 1 h, weighed for mass, sonicated for 1 h, cooled to room temperature and weighed for mass, methanol was added dropwise to make up the mass reduced by volatilization due to sonication, filtered through a microporous membrane (0.45  $\mu\text{m}$ ), and the renewed filtrate was taken to obtain the CPST test solution. HPLC analysis was implemented on an XB C18 column (4.6 mm  $\times$  250 mm, 5  $\mu\text{m}$ ). The flow rate: 1.0 mL/min, column temperature: 30  $^{\circ}\text{C}$ , the detection wavelength: 205 nm). The mobile phase is composed of solvent A (0.1% phosphoric acid-water) and solvent B (acetonitrile). Gradient method: 0 min: 10% B, 5 min: 10% B, 20 min: 30% B, 30 min: 45% B, 60 min: 55% B, 70 min : 80% B, 80 min: 80 % B. The eluent was detected and measured as follows: detector, Alltech 3300 Evaporative Light Scattering Detector (ELSD, 118 Alltech, Chicago, IL, USA), ELSD drift-tube temperature was set to 80  $^{\circ}\text{C}$ , nitrogen flow rate, 2.0 mL/min.

#### 2.5. Animals and diets

Male C57BL/6 J mice (four weeks old) supplied by Laboratory Animal Center of China Three Gorges University (Yichang, China), were used for the present study. The experimental mice were housed under a 12 h light/dark cycle and temperature and humidity controlled

environment, and food and water were supplied ad libitum, whose welfare and experimental procedures were carried out in accordance with the National Institutes of Health (Bethesda, Maryland, USA) and the related ethical regulations of China Three Gorges University. The experimental protocols were agreed by the Animal Ethics and Welfare Committee of China Three Gorges University (Permission number: CTGUAEWC-2021-085).

After a week of adaptation, the mice were randomized into five groups with 10 mice in each group including control group, high-fat diet (HFD) group (Model), HFD + CPST 25 mg/kg group (CPST-25 mg/kg), HFD + CPST 50 mg/kg group (CPST-50 mg/kg), HFD + CPST 100 mg/kg group (CPST-100 mg/kg), All drugs were administered by gavage. Mice in the control group were fed a regular diet for 8 months. In the IR and drug-treated groups, with a HFD for a similar period. In addition, giving the drug group daily therapeutic doses of CPST based on their body weight. The body weight and food intake of mice were monitored daily. We measured the IR levels 2 weeks before execution. The HFD feeding consists of 53% regular feed, 20% fructose, 5% cholesterol, 20% lard, 1% salt, 0.25% sodium chloride, and it was irradiated for sterilization.

#### 2.6. Glucose and insulin tolerance test

For oral glucose tolerance test (OGTT), after mice fasted for 16 h, body weight was weighed and recorded, and the volume of 20% glucose was calculated for each mouse by oral gavage at 2.0 g/kg, and the amount of glucose (mL) = body weight  $\times$  0.01. Blood was collected from the tail tip to measure fasting blood glucose concentration (t = 0), followed by gavage of 20% glucose solution, and blood glucose concentration was measured at different periods until the mice's blood glucose returned to 0 min when the measurement was stopped. For insulin tolerance test (ITT), briefly, mice were injected with insulin at 0.75 U/kg intraperitoneally after 4 h of fasting, and other treatments were the same as OGTT (Attia et al., 2019; Nagata et al., 2017).

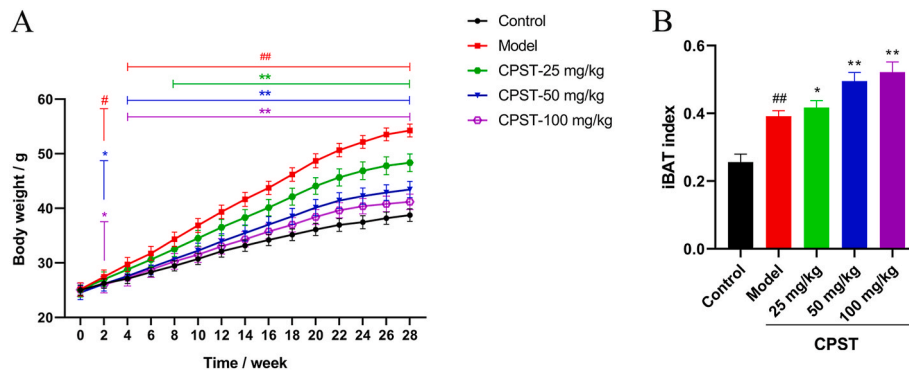


**Fig. 2.** Effect of CPST on body weight and iBAT index in the HFD mice (A) Body weight curve of mice on normal or HFD. (B) The proportion of iBAT in the overall body weight of mice. The data were shown as the mean  $\pm$  SD (n = 10). #*P* < 0.05, ##*P* < 0.01 vs. the control group. \**P* < 0.05, \*\**P* < 0.01 vs. the model group.

**2.7. Serum assays**

On the next day after the last administration, the experimental mice were anesthetized with pentobarbital sodium (50 mg/kg, *i. p.*), and blood samples were collected. The serum samples were acquired from blood and allowed to stand for 1 h at room temperature, followed by centrifugation (2000 rpm, 15 min). Aspartate aminotransferase (AST), alanine aminotransferase (ALT), creatinine (Crea), Urea nitrogen (Urea), GLUO, TG, T-CHO, HDL-C and LDL-C levels were measured with an automated clinical chemistry analyzer ADVIA-2400 (Siemens AG, German) according to the instructions.

**2.8. BAT histopathology analysis and adipocyte cross-sectional area statistics**

After collected the bloods, the experimental mouse was sacrificed, and the interscapular BAT (iBAT) was removed. The iBAT sample selected from each iBAT of the experimental mouse was fixed in 4% paraformaldehyde, dehydrated in gradient alcohol, transparent in xylene, paraffin-embedded sections with a thickness of 4  $\mu$ m, then routinely stained with hematoxylin and eosin (H&E), sealed, and observed under the light microscope. Ten adipocytes were randomly selected under the same field of view, calculated their cross-sectional areas for statistical analysis (Kim et al., 2022). The residual iBATs

were preserved at  $-80^{\circ}\text{C}$  for molecular analyses.

**2.9. Western blot analysis**

The total proteins of the iBAT were extracted by using protein extraction kits, and the protein content was measured by Multifunctional Enzyme Labeler (TECAN, Switzerland). Forty micrograms of tissue protein were transferred to PVDF membrane, and the blots were probed with primary antibodies against TLR4, MyD88, NF- $\kappa$ B, p-NF- $\kappa$ B, NLRP3, ASC, caspase-1, cleaved caspase-1, IL-18, IL-1 $\beta$ , TXNIP, GSDMD, UCP1 and  $\beta$ -actin at 4  $^{\circ}\text{C}$  overnight and then incubated with secondary antibody. The blots were developed using the ECL detection kit. Quantitative analysis was executed by using Image J Morphology Analysis System (National Institute of Health, USA), and molecular expressions were normalized to  $\beta$ -actin (Wen et al., 2011).

**2.10. Statistical analysis**

The results were expressed as mean  $\pm$  SD. Data were analyzed with SPSS 21.0 software version (SPSS Inc., Chicago, IL, USA) and GraphPad Prism 8.0.1 (Graph-Pad Software, Inc., San Diego, CA, USA), and one-way analysis of variance (ANOVA) was used for multi group comparison. Differences were considered statistically significant at *P* values less than 0.05.

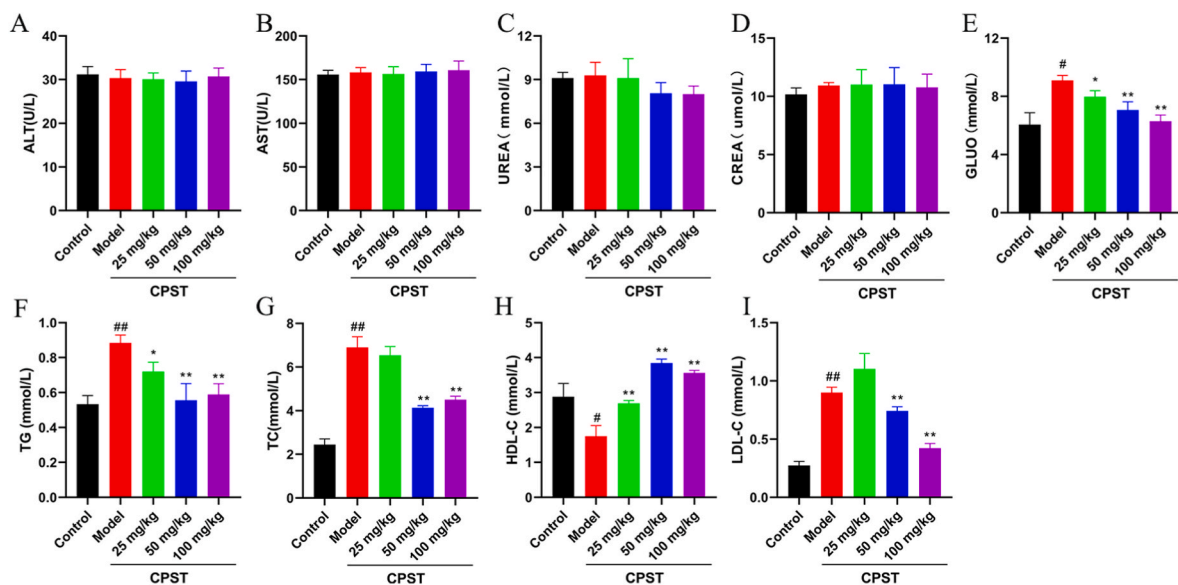


**Fig. 3.** Effect of CPST on the serum biochemical indexes of the HFD mice. (A–B) ALT and AST of the HFD mice. (C–I) Urea, Crea, GLUO, TG, T-CHO, HDL-C, LDL-C indexes of the HFD mice. The data were shown as the mean  $\pm$  SD (n = 10). #*P* < 0.05, ##*P* < 0.01 vs. the control group. \**P* < 0.05, \*\**P* < 0.01 vs. the model group.

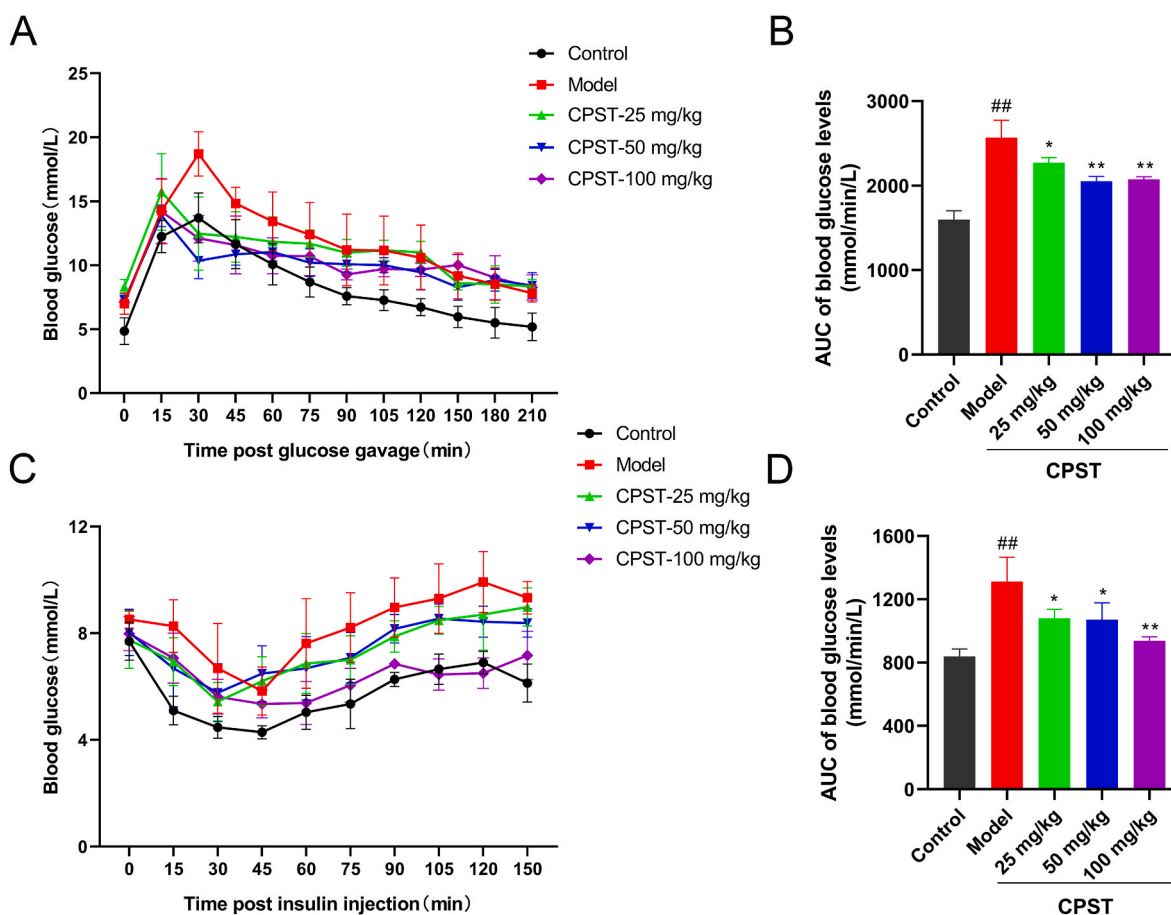


**Fig. 4.** Effects of CPST on glucose tolerance, insulin sensitivity and hyperglycemia levels in the HFD mice. (A) OGTT: Blood glucose levels were measured in mice. (B) AUC of the mean glucose levels after feeding glucose. (C) ITT: Blood glucose levels were measured in mice. (D) AUC of the mean glucose levels after insulin injection. The data were shown as the mean  $\pm$  SD ( $n = 10$ ). <sup>#</sup> $P < 0.05$ , <sup>##</sup> $P < 0.01$  vs. the control group. <sup>\*</sup> $P < 0.05$ , <sup>\*\*</sup> $P < 0.01$  vs. the model group.

### 3. Results

#### 3.1. Phytochemical analysis of CPST

Our previous verified that pterocaryoside B existed in the CPST, and Fig. 1A manifested its spectrum. The chromatographic peak corresponding to the composition at a retention time of 51 min was calibrated by pterocaryoside B control, as indicated at position P in the drawing. In Fig. 1B, the chemical structure formula of pterocaryoside B was placed, which was a moderately weak polar triterpenoid saponin with a molecular weight of 621.40026 and a strong sweet taste. The results demonstrated that the peaks in the retention time range of 40~65 min represented by pterocaryoside B. The content of it in CPST was determined, and the results manifested that the level of pterocaryoside B was 177.44 mg/g.

#### 3.2. Effect of CPST on body weight and adipose tissue index in the HFD mice

To evaluate the effect of CPST on HFD mice, we fed all mice with a HFD except control group. The administration group was given corresponding concentration of CPST by gavage. Over 8 months, their body weight changes from 0 to 28 weeks were calculated, as illustrated in Fig. 2A. Compared with the control group, the body weight of the mice in the model group was significantly more elevated, and their growth rate was higher than the control group notably ( $P < 0.01$ , respectively). After the treatment with CPST, the body mass decreased sequentially with growing doses, and the body weight growth rate declined

enormously compared with the model group ( $P < 0.05$  or  $P < 0.01$ , respectively). It was interesting to see the percentage of the different groups. As shown in Fig. 2B, the iBAT in the mice fed with HFD was remarkably lower than that of the control group ( $P < 0.01$ , respectively). After the administration of CPST treatment, the iBAT indexes were obviously reversed compared with the model group ( $P < 0.05$  or  $P < 0.01$ , respectively).

#### 3.3. Effect of CPST on serum biochemical index in the HFD mice

After 8 months of feeding, executed the mice, and collected the serum for biochemical analysis to observe the effects treated with HFD and CPST on the liver and kidney functions of mice, and to verify whether the IR model was successfully established, and investigate whether experiment drug can lower lipids and glucose. As shown in Fig. 3, the serum AST, ALT, Urea, and Crea levels of mice in the model group demonstrated no noteworthy changes compared with the control group. GLUO, LDL-C, TG, and CHOL levels were substantially higher than those in the control group ( $P < 0.01$ , respectively). In contrast, HDL-C was significantly lower than that of the control group ( $P < 0.01$ ). Abnormal changes of the aforementioned indicators were dramatically reversed after the administration of CPST ( $P < 0.05$  or  $P < 0.01$ , respectively).

#### 3.4. Effect of CPST on glucose and insulin tolerance in the HFD mice

According to the literature research, OGTT and ITT are the classic methods for assessing the ability of glucose metabolism (Attia et al.,

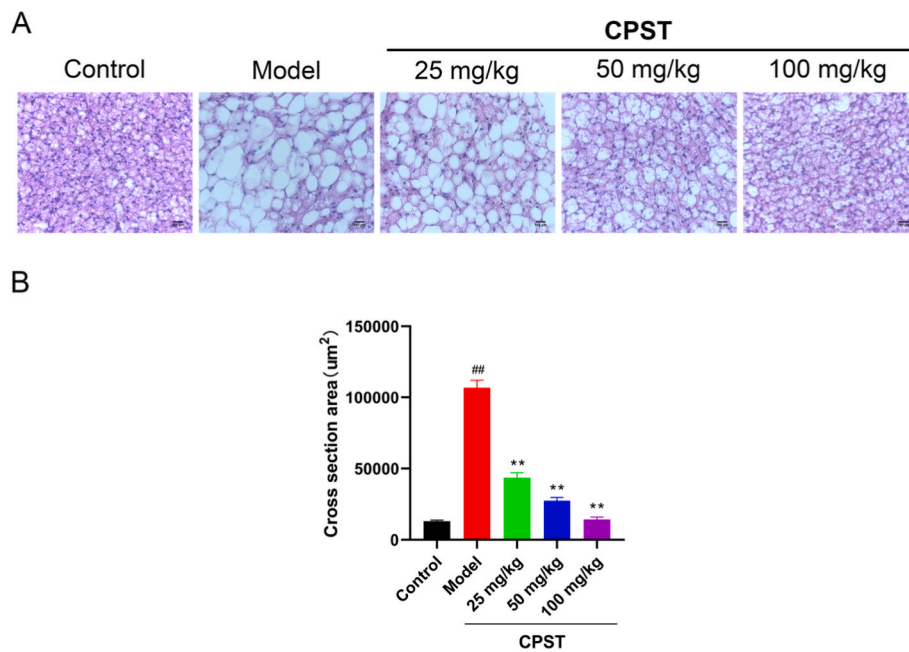


**Fig. 5.** Effect of CPST on macroscopic and microscopic histopathology of mice. (A) Representative images of hematoxylinoscopy of iBAT (scale bar = 100 μm). (B) Cross-sectional area of adipocytes by H&E staining statistics. The data were shown as the mean ± SD (n = 10). <sup>#</sup>*P* < 0.05, <sup>##</sup>*P* < 0.01 vs. the control group. <sup>\*</sup>*P* < 0.05, <sup>\*\*</sup>*P* < 0.01 vs. the model group.

2019). Therefore, to test whether the model of IR was successfully established, we carried out OGTT and ITT on C57BL/6 mice, plotted the related curves, and subsequently calculated their area under the curve (AUC) (Xu et al., 2016). As demonstrated in Fig. 4A, we noticed that after 30 min of oral glucose, the blood glucose of control mice reached its summit. It is proverbial that the body regulates the utilization of glucose by peripheral target organs through the secretion of insulin, so orally absorbed glucose will gradually metabolize, and glucose levels will drop to the initial range over time. As shown in Fig. 4B, IR mice achieved a peak of 15 min of oral glucose, and their glucose levels were

higher than those in the control group (*P* < 0.01). The area under the OGTT curve in the CPST groups indicated a dose-dependent downturn trajectory (*P* < 0.05 or *P* < 0.01, respectively). For ITT, as indicated in Fig. 4C, after injecting insulin into control mice, the glucose level dropped quickly, and then the blood glucose returned to normal level. In the model group, it decreased gradually and reached the trough value within 30 min. In terms of the AUC for ITT, as shown in Fig. 4D, the results were consistent with OGTT (*P* < 0.05 or *P* < 0.01, respectively). The data of OGTT and ITT manifested that CPST might ameliorate insulin sensitivity and glucose metabolism.

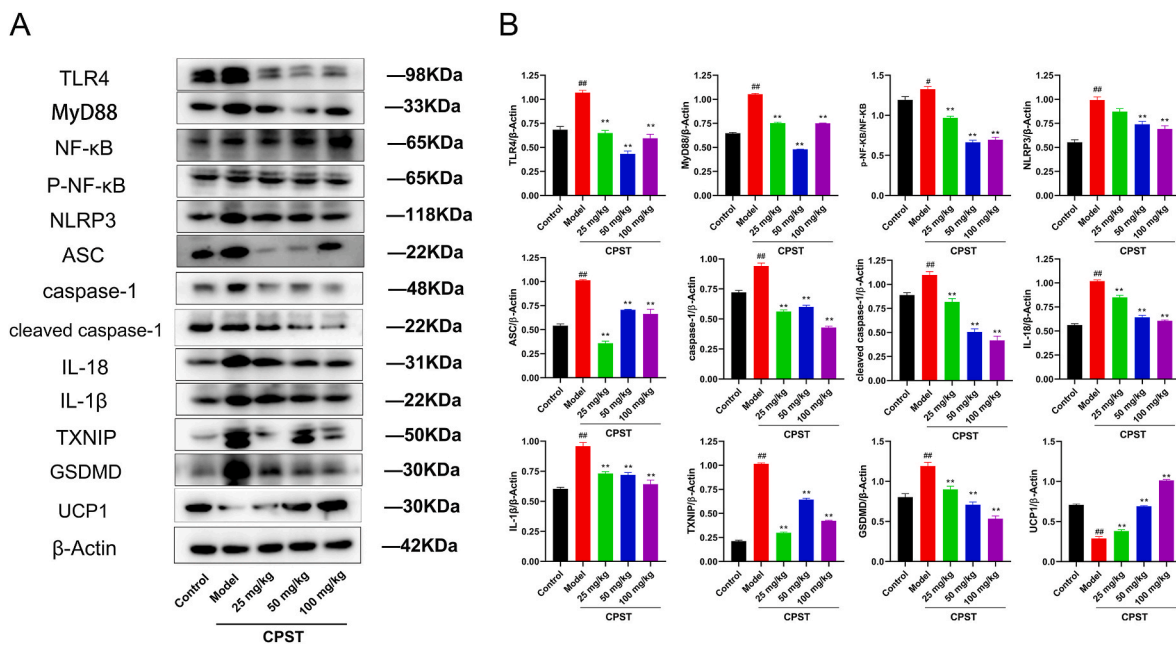


**Fig. 6.** The expression of the TLR4/NF-κB/NLRP3 inflammasome signaling pathway in iBAT. The protein expression of TLR4, MyD88, NF-κB, p-NF-κB, NLRP3, ASC, caspase-1, cleaved caspase-1, IL-18, IL-1β, TXNIP, GSDMD and UCP1 were detected in iBAT from each group mice. The data were shown as the mean ± SD (n = 4). <sup>#</sup>*P* < 0.05, <sup>##</sup>*P* < 0.01 vs. the control group. <sup>\*</sup>*P* < 0.05, <sup>\*\*</sup>*P* < 0.01 vs. the model group.

### 3.5. Effect of CPST on iBAT in the HFD mice

To observe the changes in iBAT in IR mice, we treated the slices of iBAT, then H&E staining, and observed under a microscope if they had the typical morphology and size changes following the development of IR. As shown in Fig. 5A, in the control group, all brown adipocytes were multilocular, no unilocular lipid droplet adipocytes were seen, and the adipocytes were densely distributed, while in the model group, a large number of unilocular adipocytes were distributed in brown adipocytes, and a round lipid droplet was found in the center of the cell, the iBAT was “whitening” seriously, accompanied by inflammatory infiltration, and the fat droplets were significantly larger compared with the control group ( $P < 0.01$ ). After treatment with CPST, the number of unilocular adipocytes and the volume of lipid droplets was effectively suppressed, iBATs “whitening” and inflammatory infiltration were effectively alleviated, which was further confirmed after calculating their adipocyte cross-sectional area ( $P < 0.05$  or  $P < 0.01$ , respectively) (Fig. 5B).

### 3.6. Effect of CPST on TLR4/NF- $\kappa$ B/NLRP3 inflammasome signaling pathway in the HFD mice

It has recently found that the inflammatory activation of adipose tissue and the expression and secretion of inflammatory mediators and inflammatory factors play an extremely important role in IR, while TLR4/NF- $\kappa$ B/NLRP3 inflammasome signaling pathway is closely related to this process (Sánchez-Tapia et al., 2019; Lu et al., 2022). After confirming CPST improves IR of the HFD mice, we next explored its potential mechanism through the signaling pathway. As the results shown in Fig. 6A–B, TLR4, MyD88, p-NF- $\kappa$ B/NF- $\kappa$ B, NLRP3, ASC, caspase-1, cleaved caspase-1, IL-18, IL-1 $\beta$ , TXNIP, GSDMD and UCP1 protein expressions were significantly elevated in iBAT of model group compared with control group ( $P < 0.01$ , respectively). After treated with CPST, the above protein expression levels were remarkably lowered ( $P < 0.05$  or  $P < 0.01$ , respectively). The present results were compatible with the characterization of IR, which demonstrated that the ameliorative effect of CPST on IR was associated with the inhibition of the activation of the TLR4/NF- $\kappa$ B/NLRP3 inflammasome signaling pathway.

## 4. Discussions

The leaves of *C. paliurus* is one kind of crop that has unique medicinal value and nutritional health care function, which also is a healthy food with lots of nutrients. In the folk, it is often used to clear heat, reduce swelling, stimulate saliva and quench thirst, and is known as the sugar lowering “divine tea”. Enlightened by these, we researched the structure-activity relationships and screened CPST for improving the disorders of glucolipid metabolism and relieving IR, and found that CPST was the most abundant ingredient and major active component in leaves of *C. paliurus*, which was divided into dammarane triterpene and 3,4-schicyclodane triterpenoids (Qin et al., 2016; He et al., 2021a,b; He et al., 2021). In order to further verify its improving the disorders of glucolipid metabolism and relieving IR functions, as well as the mechanisms involved, we conducted the current study. In this research, our results manifested that CPST could ameliorate HFD-induced IR, which was linked to reducing HFD-induced mice’s body weight, serum GLUO, TG, T-CHO and LDL-C, lowering the area under the oral glucose tolerance curve and insulin tolerance, elevating the percentage of brown adipose, HDL-C, reducing fat droplets of adipocytes in iBAT and cross-sectional area of adipocytes, downregulating TLR4, MyD88, NLRP3, ASC, caspase-1, cleaved caspase-1, IL-18, IL-1 $\beta$ , TXNIP, GSDMD and UCP1 protein expressions and p-NF- $\kappa$ B/NF- $\kappa$ B ratio in iBAT. Our current study manifested that CPST ameliorated HFD-induced IR by regulating TLR4/NF- $\kappa$ B/NLRP3 signaling pathway, which in turn enhancing insulin sensitivity and glucose metabolism.

IR is a metabolic disease caused by an impaired response to insulin stimulation by insulin-targeted cells such as hepatocytes, skeletal muscle

cells, and adipocytes, and its clinical manifestation is hyperinsulinemia, hyperglycemia, and hyperlipidemia (Lee et al., 2022; Xu et al., 2019). It is the basis for the development of T2D, and early intervention of IR is currently considered the most effective strategy for the treatment of T2D. In recent years, the relationship between inflammation and IR is becoming a hotspot in the study of endocrine metabolism (Greenhill, 2018). Some researchers put forward the “inflammation theory”, which suggested that inflammation was the prime mechanism of IR. In type 2 diabetes mellitus (T2DM) and obese patients, the release of inflammatory factors, such as IL-1 $\beta$ , IL-6, IL-18, TNF- $\alpha$  levels are remarkably elevated, leaving the body in a state of chronic inflammation (Al-Daghri et al., 2022; Xie et al., 2021). These results suggest that the close relationship between inflammation and IR, and intervention in inflammation is a pivotal approach to preventing and treating IR. In the present study, we found that the blood GLUO, LDL-C, TG and CHOL levels in the model mice were significantly elevated, the content of HDL-C dramatically decreased, the protein expressions of IL-1 $\beta$ , IL-18 in iBAT apparently raised. The results of OGTT and ITT also manifested that the insulin sensitivity and glucose metabolism in the model mice were significantly suppressed. On the contrary, treatment with CPST might efficiently lessen blood GLUO, LDL-C, TG and CHOL levels and the protein expressions of IL-1 $\beta$ , IL-18 in iBAT, ascend the blood HDL-C level, increase the sensitivity of HFD-induced IR mice to insulin, and enhance the metabolic capacity of glucose. The inhibitory effects of abnormal hypertrophy of adipocytes and the production of inflammatory markers in iBAT of the CPST treated groups were also similar to it. In addition, except HDL-C level, none of the above indexes in each treatment group returned to the normal level. The aforementioned results indicate that CPST could effectively reduce the expression of inflammatory factors, augment the metabolisms of blood glucose and lipids, and thus ameliorate the IR-induced by HFD. However, its therapeutic effect is less effective than the normal diet.

It is well-known that BAT is the main place of non-trembling thermogenesis in human body, and its main function is to produce heat and consume energy. When the body is stimulated by cold or fed, BAT can uncouple mitochondrial respiration mediated by UCP1, and use glucose and fatty acid as raw materials to generate heat and consume energy (Kulterer et al., 2020). Studies have shown that sustained expression of UCP1 in brown adipose tissue promotes uptake of plasma TG, while inhibiting oxidative stress and improving IR (Cheng et al., 2021; Gaspar et al., 2021). From here we see that the heat production, energy consumption and secretion of BAT have many beneficial effects on the regulation of glucose and lipid metabolism. Therefore, the effect of BAT transplantation on weight loss and improvement of glucose and lipid metabolism has become a research focus of recent scholars. Gunawardana et al. (Gunawardana and Piston, 2012). found that after subcutaneous transplantation of embryonic mouse BAT into T1DM model mice, the fasting blood glucose of mice dramatically decreased, the glucose tolerance was ameliorated, the glucose homeostasis was better, and the clinical symptoms of polydipsia and polyuria were also markedly improved. Further experiments demonstrated that BAT transplantation might better glucose metabolism, weight loss, elevate insulin sensitivity (Scheele and Wolfrum, 2020; Stanford et al., 2013; Villarroya et al., 2017). In our study, the multilocular adipocytes, more fat droplets in cytoplasm, and the remarkably increased adipocyte cross-sectional area were confirmed in the model group’s iBAT, which manifested that the brown adipocytes were severely damaged and transformed into white adipocytes, and the glucose and lipid metabolism were inhibited. After treatment with CPST, the transformation of brown adipocytes into white adipocytes was effectively reversed, the cross-sectional area of brown adipocytes was reduced, and the functions of glucose and lipid metabolism were restored. Similar to the previous results, the cross-sectional area was return to normal in each group after treatment. All the aforementioned aspects were consistent with the melioration of GLUO, LDL-C, TG, CHOL and HDL-C levels in the blood and the UCP1 protein expression in iBAT of HFD mice.

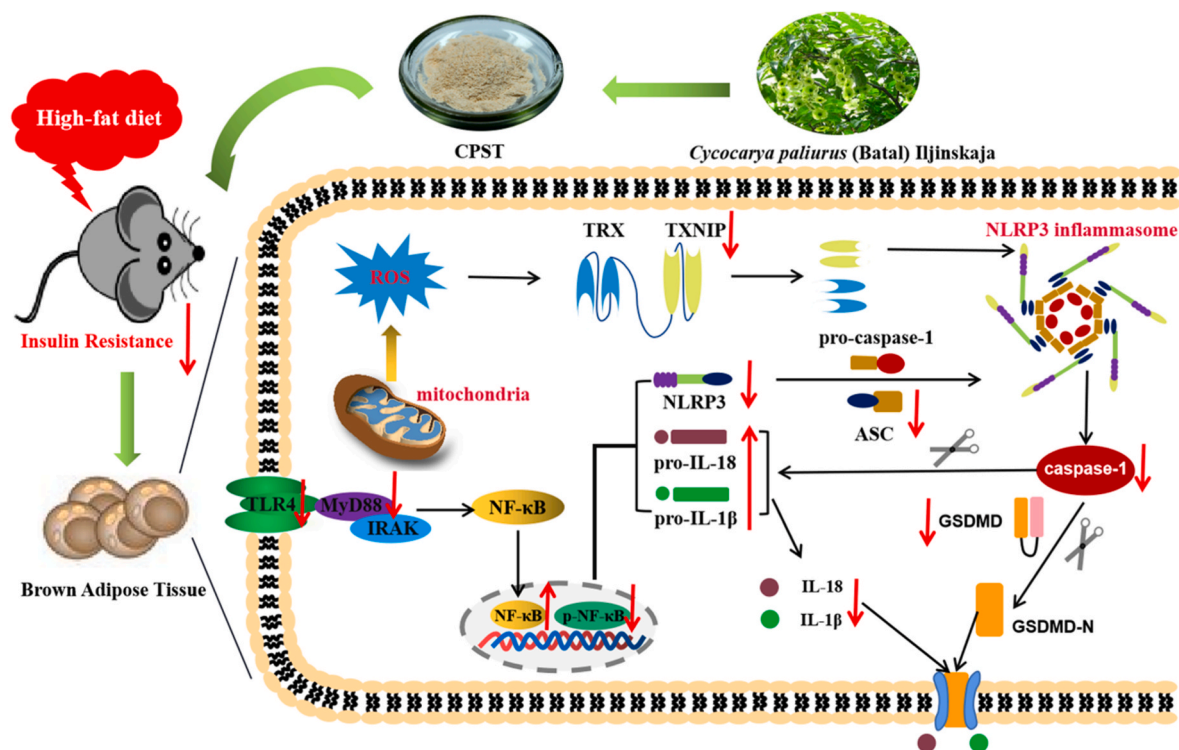


Fig. 7. Potential molecular mechanism of CPST's ameliorative effect on obesity-induced IR.

Recent studies have found that obese patients are in a low degree of chronic inflammation, their adipose tissues have a large number of inflammatory cell infiltrating, which leads to adipose tissue and IR (Kunz et al., 2021). Shankar and Gunawardana et al. (Gunawardana and Piston, 2015; Shankar et al., 2019) found that after the mice removed iBAT were fed with HFD, their adipose tissues emerged inflammatory cell infiltration and elevated serum TNF- $\alpha$ , IL-1 $\beta$ , IL-6 levels, and accompanied by obesity and IR aggravation. On the contrary, after transplantation of iBAT in HFD mice, the number of large adipocytes in adipose tissue and the destruction of cell membrane evidently decreased, the levels of serum TNF- $\alpha$ , IL-1 $\beta$ , IL-18 were obviously suppressed. The aforementioned results manifested that iBAT might play a role in reducing weight and improving IR by reducing inflammation of adipose tissue. Further research found that the TLR4, MyD88, p-NF- $\kappa$ B, TNF- $\alpha$ , IL-1 $\beta$ , IL-6 protein expressions in iBAT of obese mice induced by HFD were noticeably elevated, the apoptosis of brown adipocytes raised. In contrast, after the TLR4 gene knockout HFD mice or HFD mice are treated by Restorinol, the above protein expressions were significantly reduced, and apoptosis was restrained. The experimental results demonstrated that TLR4 gene knockout or Restorinol therapy might efficiently alleviate the chronic inflammation of iBAT in obese mice induced by HFD and improve IR by restraining TLR4/MyD88/NF- $\kappa$ B signaling pathway (Li et al., 2022; Xiao et al., 2011). In addition, the downstream NLRP3 inflammasome of this pathway also plays a crucial role in lipid metabolism and adipose tissue function, and their excessive activation equally leads to adipose tissue inflammation (Unamuno et al., 2021). Kursawe and Zhang et al. (Kursawe et al., 2016; Zhang et al., 2018) found that NLRP3, ASC, caspase-1 and IL-1 $\beta$  levels in serum and adipose tissue of T2DM patients were dramatically ascended, which confirmed that the abnormally generated glucose, FFA, saturated fatty acid and other metabolic signal molecules led to the excessive production of ROS, and induced the separation of TXNIP from thioredoxin protein (TRX), which combined with NLRP3 inflammasome, resulted in the activation of NLRP3 inflammasome (Murphy et al., 2019). Normally, the activated NLRP3 inflammasome acted on adipose tissue, liver, skeletal muscle and other tissues. In adipose tissue, NLRP3

inflammasome activation may induce self-cleavage activation of caspase-1 to become cleaved caspase-1. The cleaved caspase-1, cleaved Gasdermin D to produce the amino terminal (N-terminal) cleaving product GSDMD-N, which was located in the plasma membrane and further oligomerized. The formation of pores on the membrane led to rapid permeability of the plasma membrane, caused membrane dysfunction. The activated NLRP3 inflammasome might also interfere with the browning of white fat in the body and promote the "whitening" of brown fat, increase inflammation of adipose tissue, repress fatty acid oxidation, increase fat decomposition, and trigger IR (Benetti et al., 2013; Murphy et al., 2019). Thus it can be seen that the TLR4/NF- $\kappa$ B/NLRP3 inflammasome signaling pathway and related proteins play an important role in HFD induced IR and adipose tissue inflammation, and regulate this pathway will help to improve HFD-induced IR and restore the normal function of iBAT (Reynolds et al., 2012). In the present study, we found that the TLR4, MyD88, p-NF- $\kappa$ B/NF- $\kappa$ B, NLRP3, ASC, caspase-1, cleaved caspase-1, IL-18, IL-1 $\beta$ , TXNIP, and GSDMD protein expressions were dramatically elevated in the HFD-induced mouse iBAT. Conversely, CPST might efficiently suppress the aforementioned protein expression levels, even if the effect did not reach the extent of the control group. These current data manifested that ameliorative effect of CPST on HFD-induced IR through inhibiting the TLR4/NF- $\kappa$ B/NLRP3 inflammatory signaling pathway.

## 5. Conclusion

The present study authenticated for the first time that CPST possessed ameliorative property against HFD-induced IR, and its reformative effects were tightly related with restraining TLR4/NF- $\kappa$ B/NLRP3 inflammatory signaling pathway, thereby relieving inflammation of BATs and improving IR (Fig. 7). These data furnished new slants for elucidating the potential mechanism of CPST's ameliorative effect, and it indicated commitment in become a candidate agent to treat IR.

## CRedit authorship contribution statement

**Jie Li:** For the submission of the manuscript, the authors made different contributions to the formation of the manuscript as follows. **Junyu He:** For the submission of the manuscript, the authors made different contributions to the formation of the manuscript as follows. **Haibo He:** Resources, Data curation. **Xiao Wang:** Methodology, Experiment, Validation, Formal analysis, and, Visualization, Writing – original draft. **Shuran Zhang:** Methodology, Experiment, Validation, Formal analysis, and, Visualization, Writing – original draft. **Yumin He:** Resources, Data curation. **Jihong Zhang:** Resources, Data curation. **Chengfu Yuan:** Conceptualization, Supervision, Writing – original draft, Writing – review & editing. **HongWu Wang:** Conceptualization, Supervision, Writing – original draft, Writing – review & editing. **Daoxiang Xu:** Resources, Data curation. **Chaowang Pan:** Conceptualization, Supervision, Writing – original draft, Writing – review & editing. **Huifan Yu:** Conceptualization, Supervision, Writing – original draft, Writing – review & editing. **Kun Zou:** Conceptualization, Supervision, Writing – original draft, Writing – review & editing.

## Declaration of competing interest

The authors declare that they have no known competing financial interests or personal relationships that could have appeared to influence the work reported in this paper.

## Data availability

Data will be made available on request.

## Acknowledgements

This work was supported by the Zhejiang Basic Public Welfare Research Program (No. LGF21H090002), the Zhejiang Medical and Health Science and Technology Plan Project (No. 2022497454), the Research Foundation of Yichang City Science and Technology Bureau (No. A21-2-044. No. A18-302-a2), the Open Foundation of Hubei Key Laboratory of Wudang characteristic traditional Chinese medicine research (No. WDCM2022010) and the Natural Science Foundation of Hubei science and Technology Department (No. 2022CFB357, No. 2022CFB427).

## Abbreviations

ALT	Alanine aminotransferase.
ASC	Apoptosis associated speck like protein containing CARD.
AST	Aspartate aminotransferase.
AUC	Area under the curve.
BAT	Brown adipose tissue.
C.	<i>Paliurus Cycocarya paliurus</i> (Batal) Ilijinskaja.
CPST	Sweet triterpenoid glycoside from the leaves of <i>Cyclocarya paliurus</i> .
Crea	Creatinine
HDL-C	High-density lipoprotein cholesterol.
H&E	Hematoxylin and eosin.
HFD	High-fat diet.
HPLC	High performance liquid chromatography
iBAT	Interscapular brown adipose tissue.
IL	Interleukin.
IR	Insulin resistance.
ITT	Insulin tolerance test.
LDL-C	Low-density lipoprotein cholesterol.
MyD88	Myeloid differentiation primary response gene 88.
NF-κB	Nuclear factor κB.
NLRP3	NOD like receptor protein 3.
OGTT	Oral glucose tolerance test.

T2D	Type 2 diabetes.
T2DM	Type 2 diabetes mellitus.
TG	Triglyceride.
TLR4	Toll like receptor 4.
TNF-α	Tumor necrosis factor-α.
TRX	Thioredoxin protein.
TXNIP	Thioredoxin interacting protein.
Urea	Urea nitrogen.
UCP1	Uncoupling protein 1.
WAT	White adipose tissue.

## References

- Al-Daghri, N.M., Alokkeel, R.M.I., Alamro, A., Ansari, M.G.A., Hussain, S.D., Amer, O.E., et al., 2022. Serum asprosin levels are associated with obesity and insulin resistance in Arab adults. *J. King Saud Univ. Sci.* 34 (1), 101690 <https://doi.org/10.1016/j.jksus.2021.101690>.
- Attia, R.T., Abdel-Mottaleb, Y., Abdallah, D.M., El-Abhar, H.S., El-Maraghy, N.N., 2019. Raspberry ketone and *Garcinia Cambogia* rebalanced disrupted insulin resistance and leptin signaling in rats fed high fat fructose diet. *Biomed. Pharmacother.* 110, 500–509. <https://doi.org/10.1016/j.biopha.2018.11.079>.
- Benetti, E., Chiazza, F., Patel, N.S.A., Collino, M., 2013. The NLRP3 inflammasome as a novel player of the intercellular crosstalk in metabolic disorders. *Mediat. Inflamm.* 2013, 1–9. <https://doi.org/10.1155/2013/678627>.
- Benomar, Y., Amine, H., Crepin, D., Al, R.S., Riffault, L., Gertler, A., Taouis, M., 2016. Central resistin/TLR4 impairs adiponectin signaling, contributing to insulin and FGF21 resistance. *Diabetes* 65 (4), 913–926. <https://doi.org/10.2337/db15-1029>.
- Boström, P., Wu, J., Jedrychowski, M.P., Korde, A., Ye, L., Lo, J.C., Spiegelman, B.M., 2012. A PGC1-α-dependent myokine that drives brown-fat-like development of white fat and thermogenesis. *Nature* 481 (7382), 463–468. <https://doi.org/10.1038/nature10777>.
- Cheng, L., Wang, J.K., Dai, H., Duan, Y.H., An, Y.C., Shi, L., Zhao, B.S., 2021. Brown and beige adipose tissue: a novel therapeutic strategy for obesity and type 2 diabetes mellitus. *Adipocyte* 10 (1), 48–65. <https://doi.org/10.1080/21623945.2020.1870060>.
- Fang, Z.J., Shen, S.N., Wang, J.M., Wu, Y.J., Zhou, C.X., Mo, J.X., Gan, L.S., 2019. Triterpenoids from *Cyclocarya paliurus* that enhance glucose uptake in 3T3-L1 adipocytes. *Molecules* 24 (1). <https://doi.org/10.3390/molecules24010187>.
- Feng, Z.L., Fang, Z.J., Chen, C.T., Vong, C.T., Chen, J.L., Lou, R.H., Lin, L.G., 2021. Antihyperglycemic effects of refined fractions from *Cyclocarya paliurus* leaves on streptozotocin-induced diabetic mice. *Molecules* 26 (22). <https://doi.org/10.3390/molecules26226886>.
- Gaspar, R.C., Pauli, J.R., Shulman, G.I., Muñoz, V.R., 2021. An update on brown adipose tissue biology: a discussion of recent findings. *American Journal of Physiology-Endocrinology and Metabolism* 320 (3), E488–E495. <https://doi.org/10.1152/ajpendo.00310.2020>.
- Gonzalez-Muniesa, P., Martinez-Gonzalez, M.A., Hu, F.B., Despres, J.P., Matsuzawa, Y., Loos, R., Martinez, J.A., 2017. Obesity. *Nat. Rev. Dis. Prim.* 3, 17034 <https://doi.org/10.1038/nrdp.2017.34>.
- Greenhill, C., 2018. Mechanisms of insulin resistance. *Nat. Rev. Endocrinol.* 14 (10), 565. <https://doi.org/10.1038/s41574-018-0083-4>.
- Griffin, C., Eter, L., Lanzetta, N., Abrishami, S., Varghese, M., Mckernan, K., Singer, K., 2018. TLR4, TRIF, and MyD88 are essential for myelopoiesis and CD11c<sup>+</sup> adipose tissue macrophage production in obese mice. *J. Biol. Chem.* 293 (23), 8775–8786. <https://doi.org/10.1074/jbc.RA117.001526>.
- Gunawardana, S.C., Piston, D.W., 2012. Reversal of type 1 diabetes in mice by brown adipose tissue transplant. *Diabetes* 61 (3), 674–682. <https://doi.org/10.2337/db11-0510>.
- Gunawardana, S.C., Piston, D.W., 2015. Insulin-independent reversal of type 1 diabetes in nonobese diabetic mice with brown adipose tissue transplant. *American Journal of Physiology-Endocrinology and Metabolism* 308 (12), E1043–E1055. <https://doi.org/10.1152/ajpendo.00570.2014>.
- He, M., Chiang, H.H., Luo, H.Z., Zheng, Z.F., Qiao, Q., Wang, L., Chen, D., 2020. An acetylation switch of the NLRP3 inflammasome regulates aging-associated chronic inflammation and insulin resistance. *Cell Metabol.* 31 (3), 580–591. <https://doi.org/10.1016/j.cmet.2020.01.009>.
- He, H.B., Jiang, W.J., Zhao, D.X., Ke, Y.Q., Lu, S.G., Tang, H.B., Yin, L.Q., 2021a. Protective effects of different solvent extracts of *Cyclocarya Paliurus* against high glucose induced ins-1 cell injury. *Pharmacology and Clinics of Chinese Materia Medica* 37 (3), 113–120. <https://doi.org/10.13412/j.cnki.zyyl.2021.03.018>.
- He, H.B., Zhu, L.J., Luo, S.X., He, Y.M., Zou, K., 2021b. A review on recent research progress and future perspectives of polysaccharides from *Cyclocarya Foliium*. *Biotic Resources* 43 (2), 110–118. <https://doi.org/10.14188/j.ajsh.2021.02.002>.
- Jiang, S.L., Lin, J.Y., Zhang, Q., Liao, Y.J., Lu, F., Cai, J.R., 2022. The fates of different types of adipose tissue after transplantation in mice. *Faseb. J.* 36 (9) <https://doi.org/10.1096/fj.202200408R>.
- Jorquera, G., Russell, J., Monsalves-álvarez, M., Cruz, G., Valladares-Ide, D., Basualto-Alarcón, C., et al., 2021. NLRP3 inflammasome: potential role in obesity related low-grade inflammation and insulin resistance in skeletal muscle. *Int. J. Mol. Sci.* 22 (6), 3254. <https://doi.org/10.3390/ijms22063254>.
- Jourdan, T., Godlewski, G., Cinar, R., Bertola, A., Szanda, G., Liu, J., Kunos, G., 2013. Activation of the NLRP3 inflammasome in infiltrating macrophages by

- endocannabinoids mediates beta cell loss in type 2 diabetes. *Nat. Med.* 19 (9), 1132–1140. <https://doi.org/10.1038/nm.3265>.
- Kim, J.W., Yang, Y.M., Kwon, E.Y., Choi, J.Y., 2022. Novel plant extract ameliorates metabolic disorder through activation of brown adipose tissue in high-fat diet-induced obese mice. *Int. J. Mol. Sci.* 23 (16), 9295. <https://doi.org/10.3390/ijms23169295>.
- Kojta, I., Chacińska, M., Blachnio-Zabielska, A., 2020. Obesity, bioactive lipids, and adipose tissue inflammation in insulin resistance. *Nutrients* 12 (5), 1305. <https://doi.org/10.3390/nu12051305>.
- Kulterer, O.C., Niederstaetter, L., Herz, C.T., Haug, A.R., Bileck, A., Pils, D., Kiefer, F.W., 2020. The presence of active brown adipose tissue determines cold-induced energy expenditure and oxylipin profiles in humans. *The Journal of Clinical Endocrinology & Metabolism* 105 (7), 2203–2216. <https://doi.org/10.1210/clinem/dgaa183>.
- Kumari, M., Wang, X., Lantier, L., Lyubetskaya, A., Eguchi, J., Kang, S., Rosen, E.D., 2016. IRF3 promotes adipose inflammation and insulin resistance and represses browning. *J. Clin. Invest.* 126 (8), 2839–2854. <https://doi.org/10.1172/JCI86080>.
- Kunz, H.E., Hart, C.R., Gries, K.J., Parvizi, M., Laurenti, M., Dalla Man, C., Lanza, I.R., 2021. Adipose tissue macrophage populations and inflammation are associated with systemic inflammation and insulin resistance in obesity. *American Journal of Physiology-Endocrinology and Metabolism* 321 (1), E105–E121. <https://doi.org/10.1152/ajpendo.00070.2021>.
- Kursawe, R., Dixit, V.D., Scherer, P.E., Santoro, N., Narayan, D., Gordillo, R., Caprio, S., 2016. A role of the inflammasome in the low storage capacity of the abdominal subcutaneous adipose tissue in obese adolescents. *Diabetes* 65 (3), 610–618. <https://doi.org/10.2337/db15-1478>.
- Lee, S.H., Park, S.Y., Choi, C.S., 2022. Insulin resistance: from mechanisms to therapeutic strategies. *Diabetes & Metabolism Journal* 46 (1), 15–37. <https://doi.org/10.4093/dmj.2021.0280>.
- Li, L.N., Li, J., He, X.Q., Liu, L.L., Zhang, H.Q., Zhong, Y.L., Song, B., 2022. TLR4/MyD88/AMPK pathway involves in regulating adipose tissue inflammation and apoptosis in high-fat diet-induced obese mice. *TLR4/MyD88/AMPK. Chinese Journal of Immunology* 38 (15), 1824–1828.
- Lin, C.X., Lin, Y.Z., Xiao, J., Lan, Y.Q., Cao, Y.J., Chen, Y., 2021. Effect of momordica saponin and *Cyclocarya paliurus* polysaccharide-enriched beverages on oxidative stress and fat accumulation in *Caenorhabditis elegans*. *J. Sci. Food Agric.* 101 (8), 3366–3375. <https://doi.org/10.1002/jsfa.10966>.
- Liu, W., Deng, S.P., Zhou, D.X., Huang, Y., Li, C.G., Hao, L.L., Huang, X.S., 2020. 3,4-seco-dammarane triterpenoid saponins with anti-inflammatory activity isolated from the leaves of *Cyclocarya paliurus*. *J. Agric. Food Chem.* 68 (7), 2041–2053. <https://doi.org/10.1021/acs.jafc.9b06898>.
- Liu, X., Xie, J.H., Jia, S., Huang, L.X., Wang, Z.J., Li, C., Xie, M.Y., 2017. Immunomodulatory effects of an acetylated *Cyclocarya paliurus* polysaccharide on murine macrophages RAW264.7. *Int. J. Biol. Macromol.* 98, 576–581. <https://doi.org/10.1016/j.ijbiomac.2017.02.028>.
- Liu, Y., Cao, Y.N., Fang, S.Z., Wang, T.L., Yin, Z.Q., Shang, X.L., Fu, X.X., 2018. Antidiabetic effect of *Cyclocarya paliurus* leaves depends on the contents of antihyperglycemic flavonoids and antihyperlipidemic triterpenoids. *Molecules* 23 (5). <https://doi.org/10.3390/molecules23051042>.
- Lu, J., Zhu, D.X., Lu, J.Y., Liu, J., Wu, Z., Liu, L., 2022. Dietary supplementation with low and high polymerization inulin ameliorates adipose tissue inflammation via the TLR4/NF- $\kappa$ B pathway mediated by gut microbiota disturbance in obese dogs. *Res. Vet. Sci.* 152, 624–632. <https://doi.org/10.1016/j.rvsc.2022.09.032>.
- Monfort-Pires, M., Regeni-Silva, G., Dadson, P., Nogueira, G.A., U-Din, M., Ferreira, S.R.G., Velloso, L.A., 2022. Brown fat triglyceride content is associated with cardiovascular risk markers in adults from a tropical region. *Front. Endocrinol.* 13 <https://doi.org/10.3389/fendo.2022.919588>.
- Murphy, A.M., Smith, C.E., Murphy, L.M., Follis, J.L., Tanaka, T., Richardson, K., Roche, H.M., 2019. Potential interplay between dietary saturated fats and genetic variants of the NLRP3 inflammasome to modulate insulin resistance and diabetes risk: insights from a meta-analysis of 19 005 individuals. *Mol. Nutr. Food Res.* 63 (22), 1900226 <https://doi.org/10.1002/mnfr.201900226>.
- Nagata, N., Xu, L., Kohno, S., Ushida, Y., Aoki, Y., Umeda, R., Ota, T., 2017. Glucoraphanin ameliorates obesity and insulin resistance through adipose tissue browning and reduction of metabolic endotoxemia in mice. *Diabetes* 66 (5), 1222–1236. <https://doi.org/10.2337/db16-0662>.
- Natur, S., Damri, O., Agam, G., 2022. The effect of global warming on complex disorders (mental disorders, primary hypertension, and type 2 diabetes). *Int. J. Environ. Res. Publ. Health* 19 (15), 9398. <https://doi.org/10.3390/ijerph19159398>.
- Ono-Moore, K.D., Zhao, L., Huang, S., Kim, J., Rutkowsky, J.M., Snodgrass, R.G., Hwang, D.H., 2017. Transgenic mice with ectopic expression of constitutively active TLR4 in adipose tissues do not show impaired insulin sensitivity. *Immunity Inflammation and Disease* 5 (4), 526–540. <https://doi.org/10.1002/iid3.162>.
- Rangel-Azevedo, C., Santana-Oliveira, D.A., Miranda, C.S., Martins, F.F., Mandarim-De-Lacerda, C.A., Souza-Mello, V., 2022. Progressive brown adipocyte dysfunction: whitening and impaired nonshivering thermogenesis as long-term obesity complications. *J. Nutr. Biochem.* 105, 109002 <https://doi.org/10.1016/j.jnutbio.2022.109002>.
- Reynolds, C.M., Mcgillcuddy, F.C., Harford, K.A., Finucane, O.M., Mills, K.H.G., Roche, H.M., 2012. Dietary saturated fatty acids prime the NLRP3 inflammasome via TLR4 in dendritic cells implications for diet-induced insulin resistance. *Mol. Nutr. Food Res.* 56 (8), 1212–1222. <https://doi.org/10.1002/mnfr.201200058>.
- Roberts-Toler, C., O'Neill, B.T., Cypess, A.M., 2015. Diet-induced obesity causes insulin resistance in mouse brown adipose tissue. *Obesity* 23 (9), 1765–1770. <https://doi.org/10.1002/oby.21134>.
- Sánchez-Tapia, M., Martínez-Medina, J., Tovar, A.R., Torres, N., 2019. Natural and artificial sweeteners and high fat diet modify differential taste receptors, insulin, and TLR4-mediated inflammatory pathways in adipose tissues of rats. *Nutrients* 11 (4), 880. <https://doi.org/10.3390/nu11040880>.
- Scarano, F., Gliozzi, M., Zito, M.C., Guarnieri, L., Carresi, C., Macrì, R., et al., 2021. Potential of nutraceutical supplementation in the modulation of white and brown fat tissues in obesity associated disorders: role of inflammatory signalling. *Int. J. Mol. Sci.* 22 (7), 3351. <https://doi.org/10.3390/ijms22073351>.
- Scheele, C., Wolfrum, C., 2020. Brown adipose crosstalk in tissue plasticity and human metabolism. *Endocr. Rev.* 41 (1), 53–65. <https://doi.org/10.1210/edrv/bnz007>.
- Shankar, K., Kumar, D., Gupta, S., Varshney, S., Rajan, S., Srivastava, A., Gaikwad, A.N., 2019. Role of brown adipose tissue in modulating adipose tissue inflammation and insulin resistance in highfat diet fed mice. *Eur. J. Pharmacol.* 854, 354–364. <https://doi.org/10.1016/j.ejphar.2019.02.044>.
- Stanford, K.I., Middelbeek, R.J.W., Townsend, K.L., An, D., Nygaard, E.B., Hitchcox, K. M., Goodyear, L.J., 2013. Brown adipose tissue regulates glucose homeostasis and insulin sensitivity. *J. Clin. Invest.* 123 (1), 215–223. <https://doi.org/10.1172/JCI62308>.
- Tanase, D.M., Gosav, E.M., Costea, C.F., Ciocoiu, M., Lacatusu, C.M., Maranduta, M.A., Floria, M., 2020. The intricate relationship between Type 2 diabetes mellitus (T2DM), insulin resistance (IR), and nonalcoholic fatty liver disease (NAFLD). *J. Diabetes Res.* 2020, 1–16. <https://doi.org/10.1155/2020/3920196>.
- Unamuno, X., Gomez-Ambrosi, J., Ramirez, B., Rodriguez, A., Becerril, S., Valenti, V., Catalan, V., 2021. NLRP3 inflammasome blockade reduces adipose tissue inflammation and extracellular matrix remodeling. *Cell. Mol. Immunol.* 18 (4), 1045–1057. <https://doi.org/10.1038/s41423-019-0296-z>.
- Villarroya, F., Gavaldà-Navarro, A., Peyrou, M., Villarroya, J., Giral, M., 2017. The lives and times of brown adipokines. *Trends Endocrinol. Metabol.* 28 (12), 855–867. <https://doi.org/10.1016/j.tem.2017.10.005>.
- Wang, X.H., Li, W.Z., Kong, D., 2016. *Cyclocarya paliurus* extract alleviates diabetic nephropathy by inhibiting oxidative stress and aldose reductase. *Ren. Fail.* 38 (5), 678–685. <https://doi.org/10.3109/0886022X.2016.1155394>.
- Wang, X., Tang, L., Ping, W.X., Su, Q.F., Ouyang, S.Y., Su, J.Q., 2022. Progress in research on the alleviation of glucose metabolism disorders in type 2 diabetes using *Cyclocarya paliurus*. *Nutrients* 14 (15). <https://doi.org/10.3390/nu14153169>.
- Wang, Y.R., Cui, B.S., Han, S.W., Li, S., 2018. New dammarane triterpenoid saponins from the leaves of *Cyclocarya paliurus*. *J. Asian Nat. Prod. Res.* 20 (11), 1019–1027. <https://doi.org/10.1080/10286020.2018.1457653>.
- Wang, Y., Zheng, X.J., Li, L.Y., Wang, H., Chen, K.Y., Xu, M.J., Zhu, Y.D., 2020. *Cyclocarya paliurus* ethanol leaf extracts protect against diabetic cardiomyopathy in db/db mice via regulating PI3K/Akt/NF- $\kappa$ B signaling. *Food Nutr. Res.* 64 <https://doi.org/10.29219/fnr.v64.4267>.
- Wen, H., Gris, D., Lei, Y., Jha, S., Zhang, L., Huang, M.T., Ting, J.P., 2011. Fatty acid-induced NLRP3-ASC inflammasome activation interferes with insulin signaling. *Nat. Immunol.* 12 (5), 408–415. <https://doi.org/10.1038/ni.2022>.
- Wu, J., Boström, P., Sparks, L.M., Ye, L., Choi, J.H., Giang, A., Spiegelman, B.M., 2012. Beige adipocytes are a distinct type of thermogenic fat cell in mouse and human. *Cell* 150 (2), 366–376. <https://doi.org/10.1016/j.cell.2012.05.016>.
- Wu, T., Shen, M.Y., Guo, X.M., Huang, L.X., Yang, J., Yu, Q., Xie, J.H., 2020. *Cyclocarya paliurus* polysaccharide alleviates liver inflammation in mice via beneficial regulation of gut microbiota and TLR4/AMPK signaling pathways. *Int. J. Biol. Macromol.* 160, 164–174. <https://doi.org/10.1016/j.ijbiomac.2020.05.187>.
- Wu, T., Shen, M.Y., Yu, Q., Chen, Y., Chen, X.X., Yang, J., Xie, J.H., 2021. *Cyclocarya paliurus* polysaccharide improves metabolic function of gut microbiota by regulating short-chain fatty acids and gut microbiota composition. *Food Res. Int.* 141, 110119 <https://doi.org/10.1016/j.foodres.2021.110119>.
- Xiao, F.X., Chen, L.L., Sun, H., Shang, J., 2011. Study on the mechanism of action of resveratrol improving insulin resistance in rats fed with high fat diet. *China Journal of Hospital Pharmacy* 31 (15), 1245–1248.
- Xie, M., Tang, H.K., Li, F.F., Wu, S., Dong, Y.H., Yang, Y.D., Ma, J., 2021. Mediating roles of hsCRP, TNF- $\alpha$  and adiponectin on the associations between body fat and fatty liver disease among overweight and obese adults. *Biology* 10 (9), 895. <https://doi.org/10.3390/biology10090895>.
- Xiong, L., Ouyang, K.H., Jiang, Y., Yang, Z.W., Hu, W.B., Chen, H., Wang, W.J., 2018. Chemical composition of *Cyclocarya paliurus* polysaccharide and inflammatory effects in lipopolysaccharide-stimulated RAW264.7 macrophage. *Int. J. Biol. Macromol.* 107 (Pt B), 1898–1907. <https://doi.org/10.1016/j.ijbiomac.2017.10.055>.
- Xu, F., Zheng, X.B., Lin, B.S., Liang, H., Cai, M.Y., Cao, H.Y., Weng, J.P., 2016. Diet-induced obesity and insulin resistance are associated with brown fat degeneration in SIRT1-deficient mice. *Obesity* 24 (3), 634–642. <https://doi.org/10.1002/oby.21393>.
- Xu, L., Nagata, N., Chen, G.L., Nagashimada, M., Zhuge, F., Ni, Y.H., Ota, T., 2019. Empagliflozin reverses obesity and insulin resistance through fat browning and alternative macrophage activation in mice fed a high-fat diet. *Bmj Open Diabetes Research & Care* 7 (1), e783. <https://doi.org/10.1136/bmjdr-2019-000783>.
- Xuan, X.C., Tan, P.Z., Zhang, X.M., Huang, H., Li, Y.Z., Jiang, Y., Zhou, L.Y., 2022. Long-term low-dose alcohol intake promotes white adipose tissue browning and reduces obesity in mice. *Food Funct.* 13 (16), 8524–8541. <https://doi.org/10.1039/d2fo00743f>.
- Yu, Q.Y., Wang, T.T., Wang, F., Yang, Y., He, C.X., Yang, W.G., Zou, Z.Q., 2021. High n-3 fatty acids counteract hyperglycemia-induced insulin resistance in fat-1 mice via pre-adipocyte NLRP3 inflammasome inhibition. *Food Funct.* 12 (1), 230–240. <https://doi.org/10.1039/D0FO02092C>.
- Zhang, S.Y., Dong, Y.Q., Wang, P.C., Zhang, X.Z., Yan, Y., Sun, L.L., Jiang, C., 2018. Adipocyte-derived lysophosphatidylcholine activates adipocyte and adipose tissue macrophage nod-like receptor protein 3 inflammasomes mediating homocysteine-induced insulin resistance. *EBioMedicine* 31, 202–216. <https://doi.org/10.1016/j.ebiom.2018.04.022>.

- Zhang, Y.W., Yang, W.L., Li, W.G., Zhao, Y.J., 2021. NLRP3 inflammasome: checkpoint connecting innate and adaptive immunity in autoimmune diseases. *Front. Immunol.* 12 <https://doi.org/10.3389/fimmu.2021.732933>.
- Zhao, J.J., Wang, Z.T., Xu, D.P., Sun, X.L., 2022. Advances on *Cyclocarya paliurus* polyphenols: extraction, structures, bioactivities and future perspectives. *Food Chem.* 396, 133667 <https://doi.org/10.1016/j.foodchem.2022.133667>.
- Zhao, M., Han, Yi, Li, J.E., An, Qi, Ye, X.M., Li, Xiang, Wang, W.J., 2021. Structural characterization and antioxidant activity of an acetylated *Cyclocarya paliurus* polysaccharide (AcCPP0.1). *Int. J. Biol. Macromol.* 171, 112–122. <https://doi.org/10.1016/j.ijbiomac.2020.12.201>.
- Zhou, Q., Shi, M.Q., Wu, X.Z., He, H.B., Liu, Y., Qin, H.L., Zhang, Y.F., 2016. Protective effects of total triterpenoids extracts from *Cyclocarya paliurus* (Batal.) Iljinskaja on STZ-stimulated INS-1 cells through regulating of autophagy and apoptosis. *Chin. J. Pharmacol. Toxicol.* 30 (10), 1057–1058.